Journal of Achievements in Materials and Manufacturing Engineering
VOLUME 26
ISSUE 1
January
2008

Spectral element modelling of the thermally induced vibration of an axially moving plate

U. Lee*, K. Kwon
Department of Mechanical Engineering, Inha University, Incheon 402-751, South Korea
* Corresponding author: E-mail address: ulee@inha.ac.kr

Received 05.03.2007; published in revised form 01.01.2008

Analysis and modelling

ABSTRACT

Purpose: To develop a spectral element model for accurate prediction of the dynamic characteristics of an axially moving thin uniform plate subjected to sudden thermal loadings on its surfaces.
Design/methodology/approach: First, we have derived the governing equations of motion by using the Hamilton's principle. Secondly, we have used the wave solutions, which satisfy the governing equations of motion in the frequency domain, as the frequency-dependent shape functions to formulate the spectral element matrix by using the variational approach. Thirdly, the extremely high accuracy of the spectral element model has been evaluated by comparing the dynamic responses obtained by the spectral element analysis with the results obtained by using the conventional finite element analysis.
Findings: It has been numerically shown that the present spectral element model provides very accurate dynamic responses of an axially moving uniform plate by treating the whole plate as a single finite element, regardless of its length.
Practical implications: Numerical investigations have shown that the thermally induced vibration characteristics of an axially moving plate depends on the duration and frequency characteristics of externally applied thermal loadings as well as its moving speed.
Originality/value: The paper is the first to develop the spectral element model for the axially moving plates subjected to thermal loadings. The present spectral element model can be applied to the galvanized steel strip passing through a hot zinc tank, for instance.
Keywords: Applied mechanics; Axially moving plate; Vibration; Thermal loading; Spectral element model

1. Introduction

When a sudden thermal loading is applied to a thin-walled structure, a very rapid thermal process occurs to induce very rapid thermal deformations in the structure, thus causing the structure to vibrate. Such thermally induced vibrations may be encountered, for example, in the galvanized steel strips passing through a hot zinc tank and the high-speed modern aircrafts subjected to aerodynamic heating.

The thermally induced vibration of a beam subjected to a suddenly applied heat flux distributed along its span was studied first by Boley [1]. Since then, numerous studies have been conducted for various thermoelastic materials and structures [2-8]. Lee [9] conducted thermoelastic damping analysis for the beams, plates and shells undergoing flexural vibration, and Kinra and Milligan [10] considered thermoelastic damping for beams. Tauchert [11] presented an extensive review on the subject of thermally induced vibrations of plates, and Thornton [12] made an intensive literature survey on the thermal structures, mostly focusing on aerospace applications. To eliminate the paradox of infinite velocity of heat propagation in the classical theory of thermoelasticity, some researchers [13] developed the generalized

theory of thermoelasticity by introducing thermal relaxation times. However, as the thermal relaxation effect is very small at high temperature, the classical theory of thermoelasticity will be adopted in this study. In the existing literatures, various solution techniques have been used: they include the Green function method [14], integral transformation method [15], finite element method [2,3,5,16] and the modal analysis method [9].

The existing previous studies on the thermally induced vibration have been focused mostly on the stationary (*i.e.*, not axially-traveling) structures. Recently, Al-Huniti [17] considered the dynamics of a stationary laminated beam under the effect of a moving heat source. In the materials processing technology society, the vibrations of axially-traveling strips have been studied [18,19]. However, to the authors' best knowledge, the authors' previous work [20] seems to be the first to study the dynamics of axially-traveling thermoelastic structures such as the galvanized steel strips passing through the hot zinc tank and the present paper is the extension of the previous work [20] based on the spectral element method (SEM). The SEM is also one of element methods such as the finite element method (FEM). The key differences from FEM are as follows. In SEM, (1) the spectral element matrix (*exact* dynamic stiffness matrix), which is formulated in the frequency-domain by using the frequency-dependent dynamic shape functions, is used, and (2) the FFT algorithm is used to efficiently reconstruct the time-domain responses from the frequency-domain solutions. Because no approximation or assumption is made in the course of spectral element formulation, the SEM indeed provides exact solutions and thus it is well recognized as an *exact* solution method [21].

Thus, the purposes of this paper are: (1) to develop a spectral element model for axially moving thin uniform plates which are subjected to thermal loadings and (2) to conduct the numerical analyses to investigate the dynamic characteristics of an example axially-traveling thin plate which is subjected to a sudden heating on a part of its upper surface.

2. Dynamic equations of motion

We consider a thin uniform plate which is moving over two simply supports of distance L at a constant speed of c in its axial direction, x. The axially moving plate has small amplitude of vibration and its axial and transverse displacements don't vary significantly along its width direction, y. Thus we can define the axial and transverse displacements of strip-like plates by $U(x, t)$ and $W(x, t)$, respectively.

The equations of motion and the relevant boundary conditions of the plate can be derived from the Hamilton's principle:

$$\int_{t_1}^{t_2} \left(\delta K - \delta P + \delta W\right) dt = 0 \tag{1}$$

where K, P and δW are the kinetic energy, strain energy, and the virtual work done by external loads, respectively.

Based on the Kirchhoff's hypothesis, the displacements can be assumed as

$$\begin{aligned} W(x,t) &= w(x,t) \\ U(x,z,t) &= u(x,t) - zw'(x,t) \end{aligned} \tag{2}$$

where $w(x, t)$ is the displacement of the mid-plane of the plate in the z direction and $u(x, t)$ in the x direction. z is the transverse distance from the mid-plane to the point of interest on the cross-section of the plate. In Eq. (2), the prime ($'$) denotes the derivative with respect to the spatial coordinate x. From Eq. (2), the strain in the x direction can be readily obtained as

$$\varepsilon_{xx} = U'(x,z,t) = u'(x,t) - zw''(x,t) \tag{3}$$

The stress in the x direction, taking into account the thermal stress, is given by [9]

$$\sigma_{xx} = \frac{E}{1-\nu^2}\varepsilon_{xx} - \frac{E\alpha}{1-\nu}\Delta T(x,z,t) \tag{4}$$

where E and ν are the Young's modulus and the Poisson's ratio, respectively, α is the coefficient of thermal expansion, and $\Delta T(x, z, t)$ is the difference between the absolute temperature $T(x, z, t)$ and the reference stress-free absolute temperature T_0 as

$$\Delta T(x,z,t) = T(x,z,t) - T_0 \tag{5}$$

By using Eq. (3) and Eq. (4), the strain energy P can be derived as

$$\begin{aligned} P &= \frac{1}{2}\int_0^L \int_{-\frac{h}{2}}^{\frac{h}{2}} \sigma_{xx}\,\varepsilon_{xx}\,b\,dz\,dx \\ &= \frac{1}{2}\int_0^L \left(D\,w''^2 + \overline{EA}u'^2 + M_T\,w'' - N_T\,u'\right)dx \end{aligned} \tag{6}$$

where L is the span between two simple supports, A is the cross-sectional area of the plate, and the following definitions are used:

$$D = \frac{EI}{(1-\nu^2)}, \quad I = \frac{bh^3}{12}, \quad \overline{EA} = \frac{EA}{1-\nu^2} \tag{7}$$

where I is the area moment of inertia of the plate. In Eq. (6), M_T and N_T are the thermal moment and thermal (axial) force, respectively, defined by

$$\begin{aligned} M_T(x,t) &= \frac{E\alpha b}{1-\nu}\int_{-\frac{h}{2}}^{\frac{h}{2}} \Delta T(x,z,t)\,z\,dz \\ N_T(x,t) &= \frac{E\alpha b}{1-\nu}\int_{-\frac{h}{2}}^{\frac{h}{2}} \Delta T(x,z,t)\,dz \end{aligned} \tag{8}$$

Similarly, by using Eq. (2), the kinetic energy K can be derived as

$$K = \frac{\rho}{2}\int_0^L \left\{A(c+\dot{u})^2 + A(\dot{w}+cw')^2 + I\,\dot{w}'^2\right\} dx \tag{9}$$

where the dot ($\cdot$) denotes the derivatives with respective to the time t. The virtual work done by external loads is given by

$$\delta W = \int_0^L \{ p_x(x,t)\delta u(x,t) + p_z(x,t)\delta w(x,t)\} dx + M_1(t)\,\delta\phi_1(t) + M_2(t)\,\delta\phi_2(t) + V(t)_1\,\delta w_1(t) + V_2(t)\,\delta w_2(t) + N_1(t)\delta u_1(t) + N_2(t)\,\delta u_2(t) \quad (10)$$

where $p_x(x, t)$ and $p_z(x, t)$ are the distributed loads acting on the plate in the x and z directions, respectively. M_i, V_i and N_i (i = 1, 2) represent the boundary moments, transverse shear forces and axial forces applied at x = 0 and x = L, respectively. w_i, u_i, and ϕ_i (i = 1, 2) are the transverse displacements, axial displacements, and the slopes ($\phi = \partial w/\partial x$) defined at the boundaries. Similarly M_i, V_i, and N_i (i = 1, 2) are the bending moments, transverse shear forces, and the axial forces defined at the boundaries.

Substituting Eqs. (6), (9) and (10) into Eq. (1) and integrating by parts yields the equations of motion

$$\overline{EA}\,u'' - \rho A\,\ddot{u} = -p_x(x,t) + \frac{1}{2}N_T'$$
$$D\,w'''' + \rho A c^2\,w'' + 2\rho A c\,\dot{w}' - \rho I\,\ddot{w}'' + \rho A\,\ddot{w} = p_z(x,t) - \frac{1}{2}M_T'' \quad (11)$$

and the boundary conditions as

$$M(0,t) = -M_1(t) = 0, \quad M(L,t) = M_2(t) = 0$$
$$w(0,t) = w_1(t) = 0, \quad w(L,t) = w_2(t) = 0 \quad (12)$$
$$u(0,t) = u_1(t) = 0, \quad u(L,t) = u_2(t) = 0$$

where the following definitions are used:

$$M(x,t) = D\,w'' + \frac{1}{2}M_T$$
$$V(x,t) = -D\,w''' - \rho h c^2\,w' - \frac{1}{2}M_T' - \rho h c\,\dot{w} + \rho I\,\ddot{w}' \quad (13)$$
$$N(x,t) = \overline{EA}\,u' - \frac{1}{2}N_T$$

The temperature field T or ΔT is governed by the heat conduction equation, which can be derived from the law of energy conservation [9] as

$$-k(T'' + T^{\circ\circ}) + \rho c_p\,c\,T' + \left[\frac{T_0\,\alpha^2\,E}{1-2\nu}\left(\frac{1+\nu}{1-\nu}\right) + \rho c_p\right]\dot{T} = 0 \quad (14)$$

where the circle (°) represents the derivative with respect to z, the thickness direction, α is the coefficient of thermal expansion, k is the thermal conductivity, c_p is the specific heat at the constant strain, and c is the moving speed of the plate. Equation (14) includes the effects of the rate of thermal energy generation due to elastic deformation as well as the effect of the moving speed c of the plate. To simplify the problem, assume that the thin strip is subjected to thermal loading applied only on the top or bottom surface of the plate. Because of the geometry of the thin plate structure, the instantaneous temperature variation due to the sudden temperature change on the top or bottom surface of the plate will be more significant in the thickness direction rather than in the in-plane directions. Accordingly, one may assume the temperature as the function of only z and t to simplify Eq. (14) into the form as

$$kT^{\circ\circ} - \left(T_0\,\alpha^2\,E_\nu + \rho c_p\right)\dot{T} = 0 \quad (15)$$

where

$$E_\nu = \frac{1+\nu}{(1-2\nu)(1-\nu)}E \quad (16)$$

Notice that, because the temperature is assumed as the function of z and t only, the thermal moment M_T and the thermal force N_T defined in Eq. (8) will be the functions of t only.

3. Spectral element model

3.1. The DFT theory

By the use of DFT theory [22] a periodic function of time $x(t)$ with period T can be always expressed by the Fourier series as

$$x(t) = \sum_{n=-\infty}^{\infty} X_n\,e^{i\omega_n t} \quad (17)$$

where $i = (-1)^{1/2}$, $\omega_n = n(2\pi/T) = n\omega_1$ are the discrete frequencies, and X_n are constant Fourier (or spectral) components given by

$$X_n = \frac{1}{T}\int_0^T x(t)e^{-i\omega_n t}dt \qquad (n = 0, 1, 2, \ldots, \infty) \quad (18)$$

Equations (17) and (18) are the continuous Fourier transforms pair for a periodic function.

Although $x(t)$ is a continuous function of time t, it is often the case that only sampled values of the function are available, in the form of a discrete time series $\{x(t_r)\}$. If N is the number of samples, all equally spaced with a time interval $\Delta = T/N$, the discrete time series are given by $x_r = x(t_r)$, where $t_r = r\Delta$ and r = 0, 1, 2, …, N − 1. The integral in Eq. (18) can be replaced with the summation as follows:

$$X_n = \sum_{r=0}^{N-1} x(t_r)\,e^{-i\omega_n t_r} \qquad (n = 0, 1, 2, \ldots, N-1) \quad (19)$$

which is the discrete Fourier transform (DFT) of the discrete time series $\{x_r\}$. Any typical value x_r of the series $\{x_r\}$ can be obtained from the synthesis equation

$$x(t_r) = \frac{1}{N}\sum_{n=0}^{N-1} X_n\,e^{i\omega_n t_r} \qquad (r = 0, 1, 2, \ldots, N-1) \quad (20)$$

which is the inverse discrete Fourier transform (IDFT). Thus Eqs. (19) and (20) represent the DFT-IFFT pair. Notice that even though Eq. (19) is an approximation of Eq. (20), it allows all discrete time series $\{x_r\}$ to be regained *exactly* (Newland, 1993). The Fourier components X_n can be normally arranged as $X_{N-n} = X_n^*$ (n = 0, 1, 2, …, N/2), where X_n^* are the complex conjugates of X_n, and $X_{N/2}$ corresponds to the highest frequency $\omega_{N/2} = (N/2)\omega_1$ which is called Nyquist frequency.

The fast Fourier transforms (FFT) is an ingenious highly efficient computer algorithm which enables to perform the synthesis analysis extremely efficiently, reducing the computing time by the order $N/\log_2 N$. Notice that while the FFT-based spectral analysis uses a computer, it is not a numerical method in the usually sense, because the analytical descriptions of Eq. (18) and Eq. (19) are still retained. More details of DFT and FFT can be found in the references [22].

3.2. Formulation of spectral element model

Based on the DFT (discrete Fourier transforms) theory [22], the solutions of Eq. (5) can be assumed in the spectral forms as

$$u(x,t) = \sum_{n=0}^{N-1} U_n(x) e^{i\omega_n t}$$
$$w(x,t) = \sum_{n=0}^{N-1} W_n(x) e^{i\omega_n t} \tag{21}$$

where $U_n(x)$ and $W_n(x)$ (n = 0, 1,…, N–1) are the spectral components of $u(x,t)$ and $w(x,t)$, respectively, and N is the number of samples. Similarly, the external loads and thermal loads can be expressed in the spectral forms as

$$p_x(x,t) = \sum_{n=0}^{N-1} P_{xn}(x)\, e^{i\omega_n t}$$
$$p_z(x,t) = \sum_{n=0}^{N-1} P_{zn}(x)\, e^{i\omega_n t}$$
$$N_T(t) = \sum_{n=0}^{N-1} N_{Tn} e^{i\omega_n t} \tag{22}$$
$$M_T(t) = \sum_{n=0}^{N-1} M_{Tn} e^{i\omega_n t}$$

where $P_{xn}(x)$, $P_{zn}(x)$, N_{Tn}, and M_{Tn} (n = 0, 1,…, N-1) are the spectral components of $p_x(x,t)$, $p_y(x,t)$, $N_T(t)$, and $M_T(t)$, respectively. Notice that, because the temperature is assumed herein to be the function of z and t only, the spectral components M_{Tn} and N_{Tn} are constants, instead of being the functions of x. Substituting Eqs. (21) and (22) into Eq. (11) gives

$$\overline{EA} U_n'' + \rho A \omega_n^2 U_n = -P_{xn}$$
$$D W_n'''' + \left(\rho A c^2 + \rho I \omega_n^2\right) W_n'' + 2i\rho A c \omega_n W_n' - \rho A \omega_n^2 W_n = P_{zn} \tag{23}$$

The spectral element formulation normally begins with the homogeneous forms of governing equations without the external forces [21]. Therefore, the homogeneous form of governing equations can be reduced from Eq. (23) as

$$\overline{EA} U_n'' + \rho A \omega_n^2 U_n = 0$$
$$D W_n'''' + \left(\rho A c^2 + \rho I \omega_n^2\right) W_n'' + 2i\rho A c \omega_n W_n' - \rho A \omega_n^2 W_n = 0 \tag{24}$$

The general solutions of Eq. (24) can be assumed as follows:

$$U_n(x) = A_n e^{\kappa_n x}$$
$$W_n(x) = B_n e^{\lambda_n x} \tag{25}$$

where κ_n and λ_n denote the wavenumbers for the axial wave mode and transverse wave mode, respectively. Substituting Eq. (25) into Eq. (24) will provide two dispersion relations as

$$\overline{EA} k_n^2 + \rho A \omega_n^2 = 0$$
$$D \lambda_n^4 + \left(\rho A c^2 + \rho I \omega_n^2\right) \lambda_n^2 + 2i\rho A c \omega_n \lambda_n - \rho A \omega_n^2 = 0 \tag{26}$$

From Eq. (26), two wavenumbers k_{nr} (r =1, 2) can be obtained for the axial wave mode and four wavenumbers λ_{nr} (r =1, 2, 3, 4) for the transverse wave mode. By using the wavenumbers computed from Eq. (26), the general solutions of Eq. (24) can expressed as

$$U_n(x) = \left[\boldsymbol{E}_{Un}(x;\omega_n)\right]\{\boldsymbol{C}_n\}$$
$$W_n(x) = \left[\boldsymbol{E}_{Wn}(x;\omega_n)\right]\{\boldsymbol{C}_n\} \tag{27}$$

where

$$\left[\mathbf{E}_{Un}(x;\omega_n)\right] = \left[e^{k_{n1}x} \quad 0 \quad 0 \quad e^{k_{n2}x} \quad 0 \quad 0\right]$$
$$\left[\mathbf{E}_{Wn}(x;\omega_n)\right] = \left[0 \quad e^{\lambda_{n1}x} \quad e^{\lambda_{n2}x} \quad 0 \quad e^{\lambda_{n3}x} \quad e^{\lambda_{n4}x}\right] \tag{28}$$
$$\{\mathbf{C}_n\} = \{A_{n1} \quad B_{n1} \quad B_{n2} \quad A_{n2} \quad B_{n3} \quad B_{n4}\}^{\mathrm{T}}$$

where $\{C_n\}$ is the constant vector to be determined by boundary conditions.

Now, consider a finite strip-like plate element of length l. As shown in Figure 1, the spectral components of the nodal DOFs (spectral nodal DOFs) are defined by

$$U_{n1} = U_{n1}(0),\ W_{n1} = W_{n1}(0),\ \Phi_{n1} = W_{n1}'(0)$$
$$U_{n2} = U_{n2}(l),\ W_{n2} = W_{n2}(l),\ \Phi_{n2} = W_{n2}'(l) \tag{29}$$

Fig. 1. Sign convention for finite strip-like plate element

Applying Eq. (27) to Eq. (29) yields a relationship between the spectral nodal DOFs vector $\{d_n\}$ and the constant vector $\{C_n\}$ as follows:

$$\{\mathbf{d}_n\} = [\mathbf{X}_n(\omega_n)]\{\mathbf{C}_n\} \tag{30}$$

where

$$\{\boldsymbol{d}_n\} = \{U_{n1} \;\; W_{n1} \;\; \Phi_{n1} \;\; U_{n2} \;\; W_{n2} \;\; \Phi_{n2}\}^{\mathrm{T}}$$

$$[\boldsymbol{X}_n] = \begin{bmatrix} 1 & 0 & 0 & 1 & 0 & 0 \\ 0 & 1 & 1 & 0 & 1 & 1 \\ 0 & \lambda_{n1} & \lambda_{n2} & 0 & \lambda_{n3} & \lambda_{n4} \\ e^{k_{n1}l} & 0 & 0 & e^{k_{n2}l} & 0 & 0 \\ 0 & e^{\lambda_{n1}l} & e^{\lambda_{n2}l} & 0 & e^{\lambda_{n3}l} & e^{\lambda_{n4}l} \\ 0 & \lambda_{n1}e^{\lambda_{n1}l} & \lambda_{n2}e^{\lambda_{n2}l} & 0 & \lambda_{n3}e^{\lambda_{n3}l} & \lambda_{n4}e^{\lambda_{n4}l} \end{bmatrix} \tag{31}$$

One can eliminate the constant vector $\{C_n\}$ from Eq. (27) by using Eq. (30) to obtain

$$\begin{aligned} U_n(x) &= [\boldsymbol{E}_{Un}][\boldsymbol{X}_n]^{-1}\{\boldsymbol{d}_n\} \equiv [\boldsymbol{N}_{Un}(x;\omega_n)]\{\boldsymbol{d}_n\} \\ W_n(x) &= [\boldsymbol{E}_{Wn}][\boldsymbol{X}_n]^{-1}\{\boldsymbol{d}_n\} \equiv [\boldsymbol{N}_{Wn}(x;\omega_n)]\{\boldsymbol{d}_n\} \end{aligned} \tag{32}$$

where $[N_{Un}]$ and $[N_{Wn}]$ are the frequency-dependent dynamic shape function matrices.

The variational approach [21] is used to formulate the spectral element matrix by using the displacement fields given by Eq. (32) as well as the temperature field which will be discussed later on. The weak form statements of the governing equations (23) are given by

$$\begin{aligned} &\int_0^l \left(\overline{EA}U_n'' + \rho A\omega_n{}^2 U_n - P_{xn}\right)\delta U_n \, dx = 0 \\ &\int_0^l \left\{DW_n'''' + \left(\rho Ac^2 + \rho I\omega_n{}^2\right)W_n'' + 2i\rho Ac\omega_n W_n' \right. \\ &\qquad \left. - \rho A\omega_n{}^2 W_n - P_{zn}\right\}\delta W_n \, dx = 0 \end{aligned} \tag{33}$$

Substituting Eq. (22) into Eq. (23) may yield the spectral element equation as

$$[\mathbf{S}_n(\omega)]\{\mathbf{d}_n\} = \{\mathbf{f}_n\} \tag{34}$$

where

$$\begin{aligned} [\boldsymbol{S}_n(\omega)] &= [\boldsymbol{X}_n^{-1}]^{\mathrm{T}}([\boldsymbol{R}_{Un}] + [\boldsymbol{R}_{Wn}])[\boldsymbol{X}_n^{-1}] \\ \{\boldsymbol{f}_n\} &= \{\boldsymbol{f}_n\}_1 + \{\boldsymbol{f}_n\}_2 \end{aligned} \tag{35}$$

with the definitions

$$\begin{aligned} \{\boldsymbol{f}_n\}_1 &= \int_0^l P_{xn}(x)[\boldsymbol{N}_{Un}]^{\mathrm{T}}\,dx + \int_0^l P_{zn}(x)[\boldsymbol{N}_{Wn}]^{\mathrm{T}}\,dx \\ &\quad -\frac{1}{2}N_{Tn}[\boldsymbol{N}_{Un}(l) - \boldsymbol{N}_{Un}(0)]^{\mathrm{T}} + \frac{1}{2}M_{Tn}[\boldsymbol{N}_{Wn}'(l) - \boldsymbol{N}_{Wn}'(0)]^{\mathrm{T}} \end{aligned} \tag{36}$$

$$\{\boldsymbol{f}_n\}_2 = \{N_{1n} \;\; V_{1n} \;\; M_{1n} \;\; N_{2n} \;\; V_{2n} \;\; M_{2n}\}^{\mathrm{T}} \tag{37}$$

$$[\mathbf{R}_{Un}] = \begin{bmatrix} Y_{n11} & 0 & 0 & Y_{n14} & 0 & 0 \\ 0 & 0 & 0 & 0 & 0 & 0 \\ 0 & 0 & 0 & 0 & 0 & 0 \\ Y_{n14} & 0 & 0 & Y_{n44} & 0 & 0 \\ 0 & 0 & 0 & 0 & 0 & 0 \\ 0 & 0 & 0 & 0 & 0 & 0 \end{bmatrix} \tag{38}$$

$$[\mathbf{R}_{Wn}] = \begin{bmatrix} 0 & 0 & 0 & 0 & 0 & 0 \\ 0 & X_{n11} & X_{n12} & 0 & X_{n13} & X_{n14} \\ 0 & X_{n12} & X_{n22} & 0 & X_{n23} & X_{n24} \\ 0 & 0 & 0 & 0 & 0 & 0 \\ 0 & X_{n13} & X_{n23} & 0 & X_{n33} & X_{n34} \\ 0 & X_{n14} & X_{n24} & 0 & X_{n34} & X_{n44} \end{bmatrix} \tag{39}$$

$$Y_{nij} = \frac{e^{(k_{ni}+k_{nj})l} - 1}{k_{ni} + k_{nj}}\left(\overline{EA}k_{ni}\,k_{nj} - \rho A\omega_n{}^2\right) \tag{40}$$

$$\begin{aligned} X_{nij} = \frac{e^{(\lambda_{ni}+\lambda_{nj})l} - 1}{\lambda_{ni} + \lambda_{nj}}\{&D\lambda_{ni}^2\lambda_{nj}^2 - R_n\lambda_{ni}\lambda_{nj} \\ &+ i\rho Ac\omega_n(\lambda_{ni} - \lambda_{nj}) - \rho A\omega_n{}^2\} \end{aligned} \tag{41}$$

Spectral elements can be assembled in a completely analogous way to that used in the conventional FEM. Assembling all spectral elements represented by Eq. (34) and then applying appropriate boundary conditions may yield a global system equation. The natural frequencies can be then computed from the condition that the determinant of the global spectral stiffness matrix vanishes at natural frequencies.

The temperature field is governed by Eq. (15) and thermal boundary conditions specified on the upper and lower surfaces of plate. As done for the displacements field, the temperature field can be also represented in the spectral form and its spectral components can be obtained as

$$T_n(z) = B_{n1}e^{-\tau_n z} + B_{n2}e^{\tau_n z} \tag{42}$$

where

$$\tau_n = (1+i)\sqrt{\frac{\omega_n}{2k}\left(T_0\,\alpha^2\,E\eta + \rho c_p\right)} \tag{43}$$

The constants B_{n1} and B_{n2} are determined by the thermal boundary conditions specified on the upper and lower surfaces of plate. Once the spectral components T_n are computed from (42), the corresponding spectral components of the thermal moment M_T and the thermal force N_T in above equations can be readily computed from Eq. (22).

4. Numerical example and discussions

As an example problem, consider a thin uniform plate which is axially moving over two simple supports of distance L = 2 m as

shown in Figure 2. The plate has the thickness h = 5*mm*, width b = 0.5 m, Young's modulus E = 73 GPa, Poisson's ratio ν = 0.33, mass density ρ = 2770 kg/m^3, thermal expansion coefficient α = 23.0 $\times 10^{-6}$/K, thermal conductivity k = 177 W/mK, and the specific heat c_p = 875 J/kg·K. T_0 represents the room temperature.

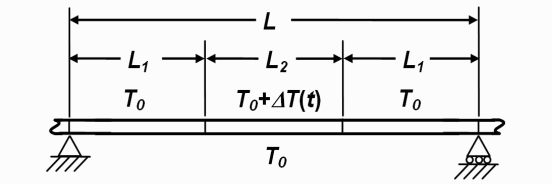

Fig. 2. An example problem: thermal boundary conditions on the upper and lower surfaces of the thin uniform strip-like plate which is axially moving over two simple supports

Table 1.
Natural frequencies (rad/s) of a thin strip-like plate

C (*m/s*)	Method	*N*	ω_1	ω_3	ω_5	ω_{15}
0	Exact [21]	·	19.37	174.31	484.22	4271.2
	SEM	1	19.37	174.31	484.16	4271.2
	FEM	10	19.37	174.41	486.14	4275.6
		20	19.37	174.32	484.35	4272.3
		50	19.37	174.31	484.23	4271.4
		100	19.37	174.31	484.23	4271.3
8	SEM	1	14.12	171.39	481.60	4271.2
	FEM	10	14.12	171.51	483.69	4275.6
		20	14.12	171.41	481.80	4272.3
		50	14.12	171.40	481.67	4271.4
		100	14.12	171.40	481.66	4271.3
12.33	SEM	1	0.00	167.33	478.07	4271.2
	FEM	10	0.00	167.47	480.32	4275.6
		20	0.00	167.35	478.28	4272.3
		50	0.00	167.34	478.14	4271.4
		100	0.00	167.34	478.13	4271.3

Note: *N* = used number of finite elements

To verify the exactness of the present spectral element model, the natural frequencies of the strip obtained by the present spectral element model (SEM), the finite element model (FEM), and the exact theory (for stationary beam, *i.e.*, c = 0 m/s) are compared in Table 1 for different moving speeds of the strip. Table 1 shows that the SEM results are identical to the exact results when c = 0 m/s, and the FEM results certainly converge to the SEM results when $c \neq$ 0 m/s as the number of finite elements used in FEM is increased. This proves the extremely high accuracy of the present spectral element model. One may observe from Table 1 that in general the natural frequencies get smaller as the moving speed increases and the fundamental natural frequency becomes zero first at about c = 12.33 m/s, at which the divergence instability occurs.

To investigate the thermally induced vibrations of the plate, the temperature on the middle part of its upper surface is suddenly heated by ΔT = 20K and the elevated temperature is sustained for o.01 seconds from t = 0 as shown in Figure 3. It is assumed that the plate is axially moving at c = 4 m/s. Figure 4 shows the thermally induced moment M_T over the region L_2 = 0.2 L on which a sudden heating is applied for 0.01 seconds.

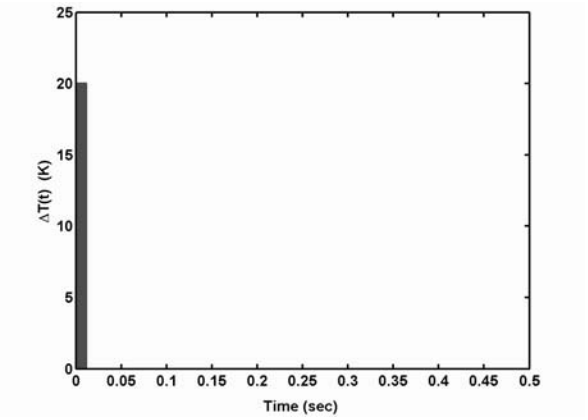

Fig. 3. Time history of the thermal load applied on the middle region (L_2) of the upper surface of plate shown in Figure 2

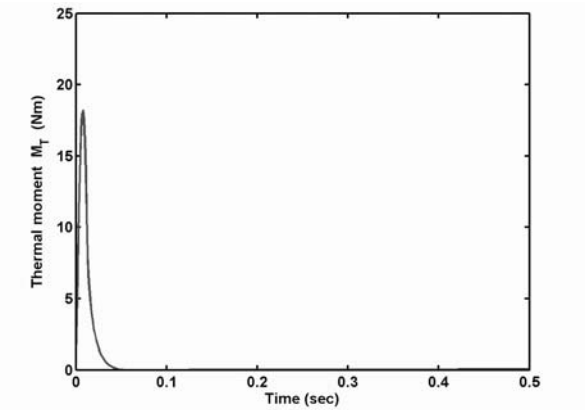

Fig. 4. Time history of the thermally induced moment (M_T) over the heating zone L_2

Figure 5 compares the frequency response functions obtained by the present SEM and FEM. Similarly Figure 6 compares the corresponding time responses. It is clear from both figures that FEM results converge to SEM results as the number of finite elements used in FEM is increased, which also proves the high accuracy of the present spectral element model. Notice that the minimum number of finite elements used in SEM is three, because the plate has temperature discontinuities at $x = L_1$ and $x = L_1 + L_2$.

Figure 6 shows the time history of the transverse vibration depending on the size of heating zone, L_2. It is found that the amplitudes of both axial and transverse vibrations become larger as L_2 is increased.

To investigate the effect of the duration of heating on the thermally induced vibration, the heating is applied on $L_2 = 0.2L$ for three different durations. As illustrated in Figure 7 for the case of transverse vibration, in general the amplitudes of both axial and transverse vibrations become larger as the duration of heating is increased.

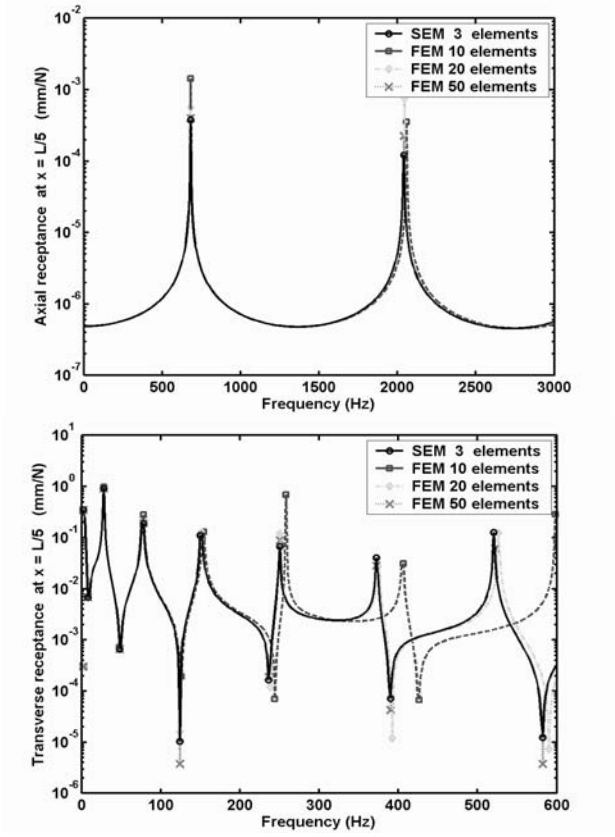

Fig. 5. Comparison of the frequency response functions of the axial and transverse displacements obtained by the present SEM and FEM when c = 4 *m/s* and $L_2 = 0.2L$

Figure 8 compares the axial and transverse vibrations induced by the harmonic thermal loading defined by $\Delta T(x,t)$ = 10 $\sin(2\pi ft)$+20 (K) when $L_2 = 0.2L$. Figure 9 shows that the resonance in transverse vibration mode occurs when the exaction frequency f is getting closer to the first transverse natural frequency (see Table 1).

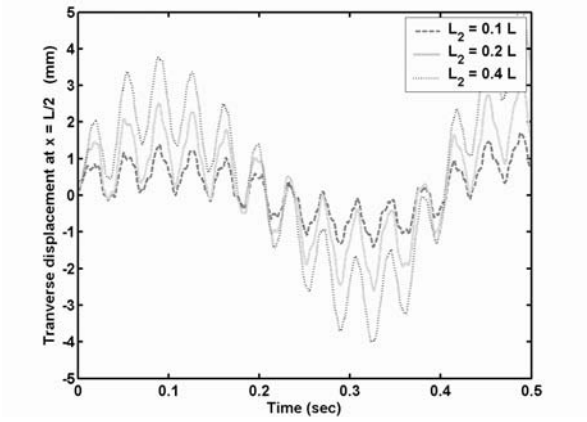

Fig. 6. Transverse vibration vs. the size of heating zone L_2

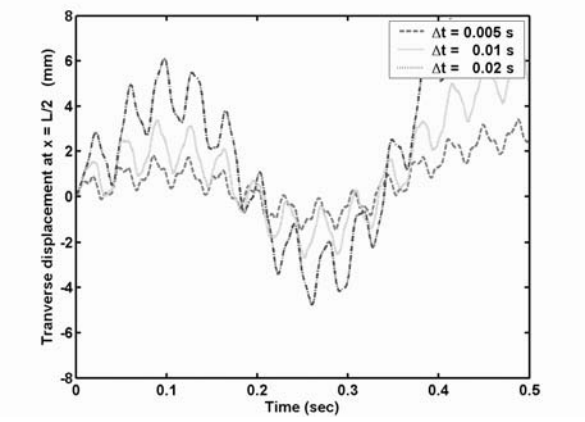

Fig. 7. Transverse vibration vs. the duration of heating Δt

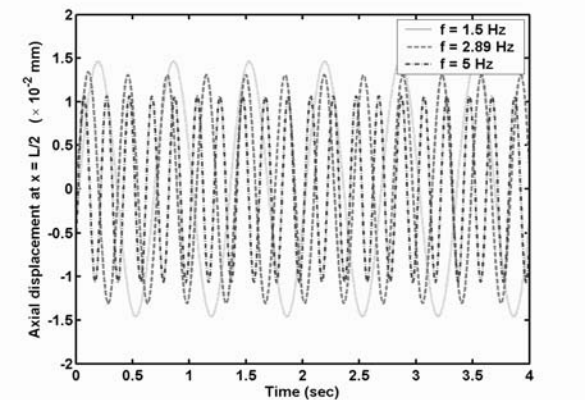

Fig. 8. Axial vibration vs. $\Delta T(x,t) = 10 \sin(2\pi ft) + 20$ (K) when $L_2 = 0.2L$

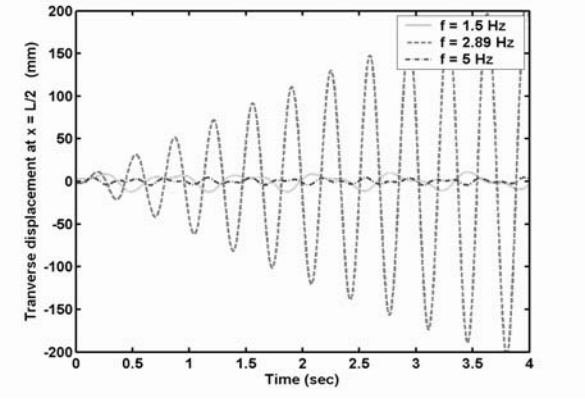

Fig. 9. Transverse vibration vs. $\Delta T(x,t) = 10 \sin(2\pi ft) + 20$ (K) when $L_2 = 0.2L$

5. Conclusions

In this paper, we have developed a spectral element model for axially moving thin strip-like plates subjected to sudden thermal

loadings on their upper or lower surface. First we have derived the governing equations of motion by using the Hamilton's principle and then have formulated the spectral element model from exact wave solutions of the governing equations of motion as the frequency-dependent shape functions by using the variational approach. The extremely high accuracy of the spectral element model has been evaluated by comparing the dynamic responses obtained by the spectral element analysis with those obtained by the conventional finite element analysis. In addition, numerical studies have been conducted to investigate the thermally induced vibrations of a strip-like plate which is axially moving over two simple supports.

Acknowledgements

This work was supported by Inha University research grant.

References

[1] B.A. Boley, Thermally induced vibrations of beams, Journal of Aeronautical Science 23 (1956) 179-181.
[2] K. Chandrashekhara, R. Tenneti, Non-linear static and dynamic analysis of heated laminated plates: a finite element approach, Composite Science and Technology 51 (1994) 85-94.
[3] W. Grzesik, M. Bartoszuk, P. Nieslony, Finite element modeling of temperature in the cutting zone in turning processes with differently coated tools, Journal of Materials Processing Technology 164-165 (2005) 1204-1211.
[4] G.D. Manolis, D.E. Beskos, Thermally induced vibrations of beam structures, Computer Methods in Applied Mechanics and Engineering 21 (1980) 337-355.
[5] H. Palaniswamy, G. Ngaile, T. Altan, Finite element simulation of magnesium alloy sheet at elevated temperatures, Journal of Materials Processing Technology 146 (2004) 52-60.
[6] H. Takuda, T. Morishita, T. Kinoshita, N. Shirakawa, Modelling of formula for flow stress of a magnesium alloy AZ31 sheet at elevated temperatures, Journal of Materials Processing Technology 164-165 (2005) 1258-1262.
[7] W.J. Xu, J.C. Fang, X.Y. Wang, T. Wang, F. Liu, Z.Y. Zhao, A numerical simulation of temperature filed in plasma -arc forming of sheet metal, Journal of Materials Processing Technology 164-165 (2005) 1644-1649.
[8] Y.Y. Yu, Thermally induced vibration and flutter of a flexible beam, Journal of Spacecraft and Rockets 6 (1969) 902-910.
[9] U. Lee, Thermal and electromagnetic damping analysis, Journal of American Institute of Aeronautics and Astronautics 23 (1985) 1784-1787.
[10] V.K. Kinra, K.B. Milligan, A second-law analysis of thermoelastic damping, Journal of Applied Mechanics 61 (1994) 71-76.
[11] T.R. Tauchert, Thermally induced flexure, buckling, and vibration of plates, Applied Mechanics Review 44 (1991) 347-360.
[12] E.A. Thornton, Thermal structures: four decades of progress, Journal of Aircraft 29 (1992) 485-498.
[13] H. Load, Y. Shulman, A generalized dynamical theory of thermoelasticty, Journal of the Mechanics and Physics of Solids 15 (1967) 299-309.
[14] J. Kidawa-Kukla, Vibration of a beam induced by harmonic motion of a heat source, Journal of Sound and Vibration 205 (1997) 213-222.
[15] J.N. Sharma, Three-dimensional vibration analysis of a homogeneous transversely isotropic thermoelastic cylindrical panel, Journal of the Acoustical Society of America 110 (2001) 254-259.
[16] N. Mukherjee, P.K. Sinha, Thermal shocks in composite plates: a coupled thermoelastic finite element analysis, Composite Structures 34 (1996) 1-12.
[17] N.S. Al-Hunti, Dynamic behavior of a laminated beam under the effect if a moving heat source, Journal of Composite Materials 38 (2004) 2143-2160.
[18] Bar, O. Bar, Types of mid-frequency vibrations appearing during the rolling mill operation, Journal of Materials Processing Technology 162-163 (2005) 461-464.
[19] J. Niziol, A. Swiatoniowski, Numerical analysis of the vertical vibration of rolling mills and their negative effect on the sheet quality, Journal of Material Processing Technology 162-163 (2005) 546-550.
[20] U. Lee, K. Kwon, Thermally induced vibration of an axially-traveling strip: spectral element analysis, Journal of Achievements in Materials and Manufacturing Engineering 17 (2006) 261-264.
[21] U. Lee, Spectral element method in structural dynamics, Inha University Press, Incheon, Korea, 2004.
[22] D.E. Newland, Random Vibrations, Spectral and wavelet analysis, Third Edition, Longman, New York, 1993.
[23] R.D. Blevins, Formulas for natural frequency and mode shape, Van Nostrand Reinhold, New York, 1979.